Halo Properties of the First $1/2^+$ State in ^{17}F from the ^{16}O$(p,\gamma)^{17}$F Reaction

R. Morlock, R. Kunz, A. Mayer, M. Jaeger, A. Müller, and J. W. Hammer
Institut für Strahlenphysik, Universität Stuttgart, Allmandring 3, D-70569 Stuttgart, Germany

P. Mohr and H. Oberhummer
Institut für Kernphysik, Technische Universität Wien, Wiedner Hauptstraße 8-10, A-1040 Wien, Austria

G. Staudt and V. Kölle
Physikalisches Institut, Universität Tübingen, Auf der Morgenstelle 14, D-72076 Tübingen, Germany
(Received 3 July 1997)

The capture cross section of the reaction ^{16}O$(p,\gamma)^{17}$F was measured in the energy range from $E_{\text{c.m.}} = 200-3750$ keV using the windowless gas target facility RHINOCEROS. The low-energy S factor that is dominated by the transition to the $1/2^+$ first excited state in ^{17}F increases strikingly with decreasing energy. This behavior is explained by the halo properties of this $1/2^+$ state within the framework of the direct capture model. [S0031-9007(97)04445-1]

PACS numbers: 25.40.Lw, 21.10.Pc, 26.20.+f, 27.20.+n

Hydrogen burning of second-generation stars mainly takes place via the proton-proton (pp) chain and the CNO cycle. These are nuclear reaction networks leading, as a final result, to the fusion of four protons into helium and being responsible for the energy production of these stars. A changeover from the pp chain to the CNO cycle is observed near $T \approx 2 \times 10^7$ K. The reaction ^{16}O$(p,\gamma)^{17}$F is a link to the higher branches of the CNO cycle. Exact knowledge of the reaction rate is necessary for the modeling of nucleosynthesis in the hydrogen-burning stars.

Up to now there exist some measurements of this reaction close to the energy range of astrophysical interest [1–5], most of them carried out using solid state targets. The data of Rolfs *et al.* [4] which cover the widest energy range up to now had to be calibrated to the older experiment of Tanner [3]. Furthermore, some of the previous experiments did not distinguish between transitions into the $5/2^+$ ground state and the $1/2^+$ first excited state of ^{17}F.

Now a new experiment has been performed covering an energy range between $E_{\text{c.m.}} = 200$ keV to $E_{\text{c.m.}} = 3750$ keV. In this range only two resonances at $E_{\text{c.m.}}(1/2^-) = 2504$ keV [$E_x(1/2^-) = 3104$ keV] and $E_{\text{c.m.}}(5/2^-) = 3257$ keV [$E_x(5/2^-) = 3857$ keV] are found. That means that the reaction proceeds mainly by the direct capture (DC) of a p-wave proton into the ground state (DC $\rightarrow 5/2^+$) and the first excited state (DC $\rightarrow 1/2^+$).

The beam was provided by the 4 MV Dynamitron accelerator of the Institut für Strahlenphysik, Universität Stuttgart. Ion beams of H^+ (10–70 μA), H_2^+ (15–45 μA), and H_3^+ (35–70 μA) have been used. The energy broadening due to the Coulomb explosion of the molecular ions did not affect the measurement. The experiment was carried out using the differentially pumped gas target system RHINOCEROS which is operated windowless and recirculating. The gas used was isotopically enriched in ^{16}O to a degree of 99.99% (purchased from IC Chemikalien, Munich, Germany). The reaction chamber is a flat cell with four ports radiating from the center of the chamber. These ports are used for gas inlet and for the supply of an electronic manometer and two particle detectors. The chamber has an effective length of about 6 cm. The gas pressure was 5.7 mbar, it corresponds to an effective target thickness of 14.5 keV ($E_{\text{p,lab}} = 200$ keV), 5.6 keV ($E_{\text{p,lab}} = 1$ MeV), and 2.1 keV ($E_{\text{p,lab}} = 4$ MeV). To avoid background reactions all inner surfaces are plated with a gold layer of about 20 μm thickness. The particle beam was dumped in a Faraday cup about 150 cm behind the reaction chamber. Typical measuring times were between some minutes at higher energies and up to 2 days at the lowest energies.

Two particle detectors have been used to monitor the primary intensity by observing the elastically scattered protons at the angles $\vartheta_{\text{lab}} = 90°$ and $\vartheta_{\text{lab}} = 120°$. The elastic scattering is following the Rutherford law only at the lowest energies, and therefore in a separate experiment we measured the elastic scattering excitation function by using mixtures of oxygen with krypton and oxygen with xenon, and by assuming pure Rutherford scattering on the heavy noble gases. The results are shown in Fig. 1.

Two γ detectors were placed on both sides of the reaction chamber, one at $\vartheta_{\text{lab}} = 90°$ and the other at $\vartheta_{\text{lab}} = 55°$, both as close as possible to the reaction chamber to achieve large solid angles. Both high-purity germanium (HPGe) detectors have a relative efficiency of 100% (compared to a 3×3 in. NaI detector). For background reduction both detectors were surrounded by an active BGO shield. The observed γ spectra (see Fig. 2) are characterized by the transitions DC $\rightarrow 5/2^+$ and DC $\rightarrow 1/2^+$. In the insets of Fig. 2 the yield curves are shown for both transitions.

The measured yield was converted to the astrophysical S factor taking into account: (i) the energy loss and

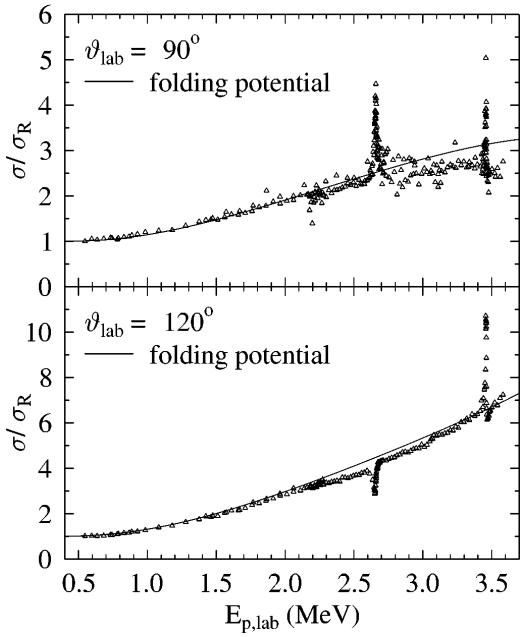

FIG. 1. Elastic scattering excitation functions of $^{16}O(p,p)^{16}O$ at $\vartheta_{lab} = 90°$ (upper diagram) and $\vartheta_{lab} = 120°$ (lower diagram). The lines are the result of an optical model calculation with a potential strength adjusted to the binding energies of the $5/2^+$ ground state and $1/2^+$ first excited state for the L = even partial waves and $\lambda = 1$ for the L = odd partial waves.

straggling of the protons in the extended gas target and the energy width of the accelerator, (ii) the solid angle of the HPGe detectors, (iii) the angular distribution of the emitted γ rays [4], and (iv) the dependence of the detection efficiency on the γ-ray energy, emission position, and emission angle. The efficiency was determined using the code GEANT [6], and the GEANT calculations were confirmed by efficiency measurements using calibration sources. The results of the $^{16}O(p,\gamma)^{17}F$ experiment are shown in Fig. 3. The lowest data point for the transition to the first excited $1/2^+$ state $S(E_{c.m.} = 221\ \text{keV}) = 6.31$ keVb corresponds to a cross section of only 2.16 nb which has to be measured at a transition energy of $E_\gamma = 326$ keV (the numerical data are available from the authors).

The theoretical analysis of the experimental data was performed in the framework of the direct capture model. The DC cross section σ_i^{DC} for each final state i is determined by the square of the overlap of the scattering wave function $\chi_l(r)$, the electromagnetic transition operators $\mathcal{O}^{E\mathcal{L}/M\mathcal{L}}$, and the bound state wave function $u_{NL,i}(r)$, and by the spectroscopic factors C^2S_i of the final states [4,7,8]:

$$\sigma_i^{DC} \sim C^2S_i |\langle u_{NL,i}(r)\,|\mathcal{O}^{E\mathcal{L}/M\mathcal{L}}\,|\chi_l(r)\rangle|^2, \qquad (1)$$

where N and L are the node number and the angular momentum number of the final state wave function which are related to the oscillator quantum number Q by

$$Q = 2N + L\,. \qquad (2)$$

Assuming an inert ^{16}O core the $5/2^+$ ground state and the $1/2^+$ first excited state in ^{17}F have pure single-particle configurations: $C^2S(5/2^+) = 1$ and $C^2S(1/2^+) = 1$. These values are in good agreement with shell model calculations [9] and with many transfer experiments (see Refs. [9,10]). We adopt for the following calculations $C^2S(5/2^+) = 1$ and $C^2S(1/2^+) = 1$.

For the calculation of the scattering and bound state wave functions we use systematic folding potentials [11,12]

$$V_F(r) = \int\int \rho_P(r_P)\rho_T(r_T) \times v_{eff}(E, \rho = \rho_P + \rho_T, s = |\vec{r} + \vec{r_P} - \vec{r_T}|) \times d^3r_P\, d^3r_T\,, \qquad (3)$$

where ρ_P, ρ_T are the densities of projectile and target, respectively, which are taken from electron scattering

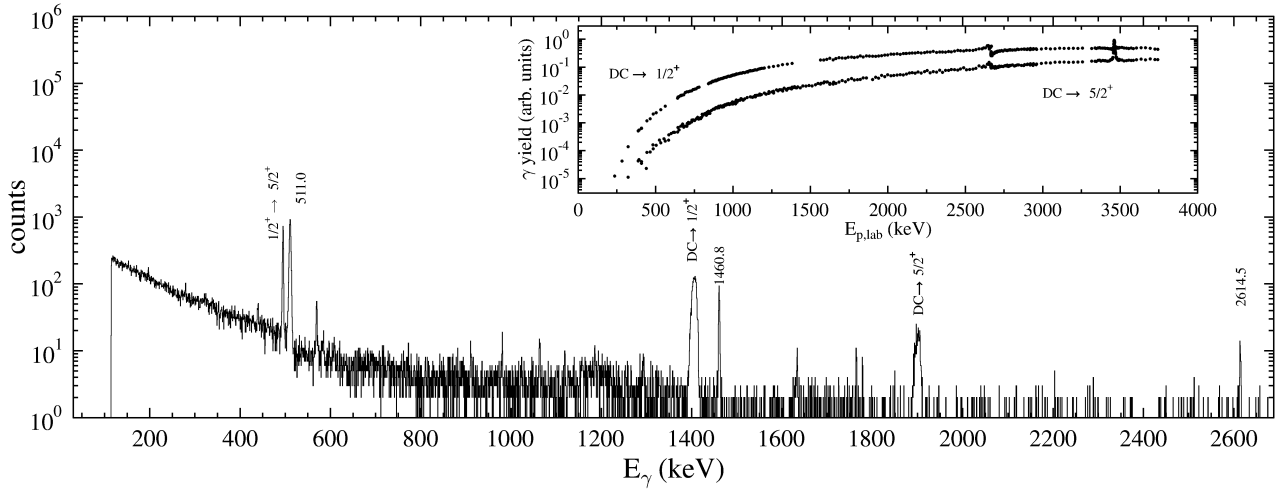

FIG. 2. γ-ray spectrum of the HPGe detector placed at $\vartheta_{lab} = 90°$ for $E_{p,lab} = 1400$ keV. In the inset the experimental γ-ray yield of the reactions $^{16}O(p,\gamma_0)^{17}F$ $(5/2^+)$ and $^{16}O(p,\gamma_1)^{17}F$ $(1/2^+)$ is shown for this detector.

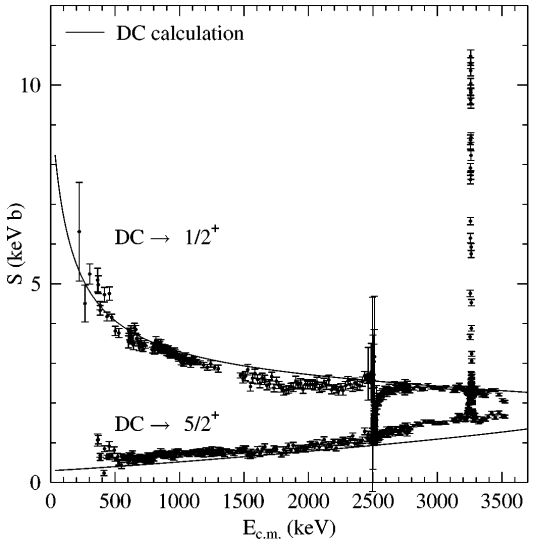

FIG. 3. Experimental capture cross section of the reactions $^{16}\mathrm{O}(p,\gamma_0)^{17}\mathrm{F}$ and $^{16}\mathrm{O}(p,\gamma_1)^{17}\mathrm{F}$ compared to a DC calculation. Note the strikingly different branching ratio between DC $\rightarrow 5/2^+$ and DC $\rightarrow 1/2^+$.

experiments [13], and v_{eff} is the effective nucleon-nucleon interaction taken in the well-established DDM3Y parametrization [11,12]. Details about the folding procedure can be found in Ref. [14]; the folding integral in Eq. (3) was calculated using the code DFOLD [15]. The volume integral per interacting nucleon pair is $J_{\mathrm{R}} = 525.93$ MeV fm^3, and the root-mean-square radius is $r_{\mathrm{F,rms}} = 3.311$ fm. The optical potential is given by

$$V(r) = \lambda V_{\mathrm{F}}(r) + \lambda_{\mathrm{s.o.}} \frac{4}{r} \frac{dV_{\mathrm{F}}}{dr} \vec{L}\vec{S} + V_{\mathrm{C}}(r), \quad (4)$$

with the potential strength parameter λ which is close to unity, and the Coulomb potential $V_{\mathrm{C}}(r)$ which is taken in the usual form of a homogeneously charged sphere with the Coulomb radius $R_{\mathrm{C}} = r_{\mathrm{F,rms}}$. Additionally, a weak spin–orbit potential is used with the usual Thomas form proportional to dV/dr and a spin–orbit strength parameter $\lambda_{\mathrm{s.o.}}$.

For the $L =$ even partial waves the parameters λ and $\lambda_{\mathrm{s.o.}}$ are adjusted to reproduce the binding energies of the $5/2^+$ ground state ($E_{\mathrm{B}} = -600.5$ keV, $Q = 2$, $N = 0$, $L = 2$) and of the $1/2^+$ first excited state ($E_{\mathrm{B}} = -105.1$ keV, $Q = 2$, $N = 1$, $L = 0$): $\lambda = 1.0976$ and $\lambda_{\mathrm{s.o.}} = -0.1757$ fm^2. This potential also describes the broad $3/2^+$ state at $E_x = 5.0$ MeV in ^{17}F; the $5/2^+$ ground state and the $3/2^+$ state are the two dominating $L = 2$ states in ^{17}F. For the $L =$ odd partial waves we use the bare folding potential [$\lambda(L = \mathrm{odd}) = 1$] and the same spin-orbit coupling as for the even partial waves. This choice of the potential parameters is confirmed by the good description of the experimental $^{16}\mathrm{O}(p,p)^{16}\mathrm{O}$ elastic scattering excitation function at $\vartheta_{\mathrm{lab}} = 90°$ and $\vartheta_{\mathrm{lab}} = 120°$ (see Fig. 1).

Both transitions to the $5/2^+$ ground state and to the $1/2^+$ state are dominated by E1 transitions from the incoming p wave to the bound d ($5/2^+$) and s waves ($1/2^+$). We took into account all possible E1, E2, and M1 transitions from the incoming s, p, d, f, and g waves, but beside the mentioned E1 transitions from the incoming p wave only the E1 transition from the incoming f wave to the bound d wave gives a significant contribution at higher energies.

With the exception of the $1/2^-$ and $5/2^-$ resonances at $E_{\mathrm{c.m.}}(1/2^-) = 2504$ keV [$E_x(1/2^-) = 3104$ keV] and $E_{\mathrm{c.m.}}(5/2^-) = 3257$ keV [$E_x(5/2^-) = 3857$ keV] a very good agreement between the experimental capture data and the calculation is obtained (see Fig. 3). These resonances do not have a dominating $^{16}\mathrm{O} \otimes p$ configuration. They are not included in the model space of this simple two–body model of ^{17}F.

It has to be pointed out that the nonresonant capture cross section is *predicted* independently by the DC model; *the calculations are not adjusted to the experimental capture data.*

On the first view a surprising energy dependence of the branching ratio of the transitions to the ground state and to the first excited state can be seen in Fig. 3. To the best of our knowledge these facts were not noticed in any previous paper. The ground state transition shows the expected behavior. To be captured the incoming p-wave proton has to tunnel through both the Coulomb and the centrifugal barrier. As a consequence the S factor decreases to lower energies because the definition of the S factor $S(E) = E \exp(2\pi\eta)\,\sigma(E)$ takes into account only the tunneling through the Coulomb barrier.

The increase of the S factor for the transition to the $1/2^+$ state is a consequence of the halo properties of the $1/2^+$ bound state wave function. Because of the very small binding energy ($E_{\mathrm{B}} = -105.13$ keV) the bound state wave function has a very long tail. The root-mean-square radii r_{rms} defined by

$$r_{\mathrm{rms}}^2 = \int_0^\infty r^2 u^2(r)\, dr \quad (5)$$

are $r_{\mathrm{rms}}(5/2^+) = 3.698$ fm and $r_{\mathrm{rms}}(1/2^+) = 5.333$ fm, respectively. The large radius of the $1/2^+$ bound state in ^{17}F also leads to the anomalously large displacement energy [16] and to an enhanced B(E2) value [17].

In Fig. 4 the real part of the integrand of the overlap integral in Eq. (1) is shown for both E1 transitions from the incoming p wave to the bound s and d waves at the energies $E_{\mathrm{c.m.}} = 0.1$ MeV and $E_{\mathrm{c.m.}} = 1.0$ MeV. (The imaginary part of the integrand is proportional to the real part when a real potential is used for the calculation of the optical wave functions.) As one can see the main contribution for the transition to the $1/2^+$ state is shifted towards larger radii when the energy decreases. At $E_{\mathrm{c.m.}} = 0.1$ MeV *the main contribution for the transition to the* $1/2^+$ *halo state comes from about* $r \approx 50$ *fm.* Consequently, the proton can be captured far outside the classical nuclear radius [$R_{\mathrm{class}} \approx (1.3\ \mathrm{fm}) A_{\mathrm{T}}^{1/3} = 3.276$ fm] without tunneling through the full Coulomb and centrifugal barrier. This

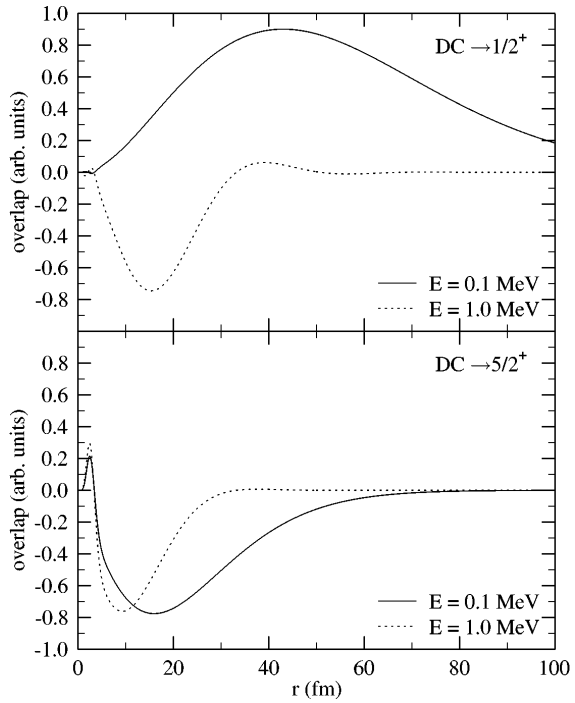

FIG. 4. Radial dependence (in arbitrary units) of the real part of the integrand in the overlap integral in Eq. (1) at the energies $E_{\mathrm{c.m.}} = 0.1$ MeV (full line) and $E_{\mathrm{c.m.}} = 1.0$ MeV (dashed line) for the transitions DC $\rightarrow 5/2^+$ and DC $\rightarrow 1/2^+$.

halo effect is the reason for the increasing S factor at low energies. In contrast to other capture reactions of astrophysical interest, e.g., $^{12}\mathrm{C}(\alpha,\gamma)^{16}\mathrm{O}$, in this case the increasing S factor is *not* a consequence of a subthreshold resonance, and electron screening which could also increase the S factor at low energies is negligible in the energy range of this experiment.

Because the capture process to the $1/2^+$ state happens far outside the range of the nuclear potential the influence of the nuclear potential on the capture cross section is very weak. For example, at the solar temperature ($T_6 = 15$ corresponding to a Gamow window at $E_{\mathrm{c.m.}} = 29$ keV) a potential strength increased or decreased by 10% for the $L =$ odd partial waves leads to a S factor increased or decreased by less than 0.2%. This fact was already pointed out by Brune [18] who obtained similar results for the E1 transition to the $1/2^+$ final state using a Woods-Saxon potential which was adjusted to reproduce the binding energy of the $1/2^+$ state. As expected, the calculation of the capture cross section to the $5/2^+$ ground state is more sensitive to the optical potential, especially at higher energies where the capture process occurs at smaller distances. However, at astrophysically relevant energies the dependence on the potential strength becomes small again.

The astrophysical reaction rate factor $N_A\langle\sigma \cdot v\rangle$ obtained from the new experimental data and the theoretical extrapolation to lower energies agrees surprisingly well with the adopted rate by Caughlan and Fowler [19]. In that work an increasing S factor towards lower energies was assumed without any experimental confirmation or theoretical explanation.

In conclusion, the $^{16}\mathrm{O}(p,\gamma)^{17}\mathrm{F}$ capture cross section was measured in the energy range from $E_{\mathrm{c.m.}} = 200$–3750 keV over 5 orders of magnitude using the windowless gas target facility RHINOCEROS. The experimental data show a strikingly different energy dependence of the branching ratio between the transition to the $5/2^+$ ground state and to the $1/2^+$ first excited state of $^{17}\mathrm{F}$ which is bound by only 105 keV. This effect which was not noticed in previous work can be explained theoretically by the halo properties of the $1/2^+$ state using the direct capture model.

We thank Professor Dr. U. Kneißl for supporting this investigation. We also recognize the work of the dynamitron team, head H. Hollick, who provided the different beams. We would like to thank Professor Dr. R. Santo, Münster, for lending us the BGO crystals. This work was supported by the Deutsche Forschungsgemeinschaft (DFG Projects No. Ha 962 and No. Mo739) and Fonds zur Förderung der wissenschaftlichen Forschung (FWF Project No. S7307–AST).

[1] J. B. Warren, K. A. Laurie, D. B. James, and K. L. Erdman, Can. J. Phys. **32**, 563 (1954).
[2] R. H. Hester, R. E. Pixley, and W. A. Lamb, Phys. Rev. **111**, 104 (1958).
[3] N. Tanner, Phys. Rev. **114**, 1060 (1959).
[4] C. Rolfs, Nucl. Phys. **A217**, 29 (1973).
[5] H. C. Chow, G. M. Griffith, and T. H. Hall, Can. J. Phys. **53**, 1672 (1975).
[6] R. Brun and F. Carminati, GEANT Detector Description and Simulation Tool, CERN Program Library Long Writeup W5013 edition, CERN, Geneva, Switzerland, 1993.
[7] B. T. Kim, T. Izumoto, and K. Nagatani, Phys. Rev. C **23**, 33 (1981).
[8] K. H. Kim, M. H. Park, and B. T. Kim, Phys. Rev. C **35**, 363 (1987).
[9] J. Vernotte, G. Berrier-Ronsin, J. Kalifa, R. Tamisier, and B. H. Wildenthal, Nucl. Phys. **A571**, 1 (1994).
[10] M. Yasue *et al.*, Phys. Rev. C **46**, 1242 (1992).
[11] G. R. Satchler and W. G. Love, Phys. Rep. **55**, 183 (1979).
[12] A. M. Kobos, B. A. Brown, R. Lindsay, and R. Satchler, Nucl. Phys. **A425**, 205 (1984).
[13] H. de Vries, C. W. de Jager, and C. de Vries, At. Data Nucl. Data Tables **36**, 495 (1987).
[14] H. Abele and G. Staudt, Phys. Rev. C **47**, 742 (1993).
[15] H. Abele, Univ. Tübingen, computer code DFOLD (unpublished).
[16] J. A. Nolen, Jr. and J. P. Schiffer, Annu. Rev. Nucl. Sci. **19**, 471 (1969).
[17] B. A. Brown, A. Arima, and J. B. McGrory, Nucl. Phys. **A277**, 77 (1977).
[18] C. R. Brune, Nucl. Phys. **A596**, 122 (1996).
[19] G. R. Caughlan and W. A. Fowler, At. Data Nucl. Data Tables **40**, 283 (1988).